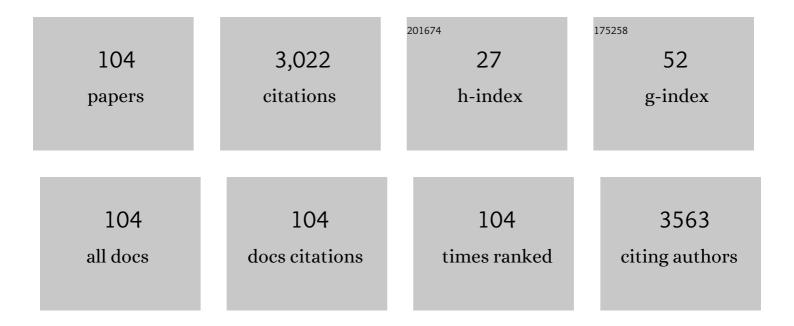
## André Santarosa Ferlauto

List of Publications by Year in descending order

Source: https://exaly.com/author-pdf/8644275/publications.pdf Version: 2024-02-01



#	Article	IF	CITATIONS
1	Chemical vapor deposition graphene transfer onto asymmetric <scp>PMMA</scp> support. Journal of Applied Polymer Science, 2022, 139, 51590.	2.6	2
2	Aerosol-Printed MoS <sub>2</sub> Ink as a High Sensitivity Humidity Sensor. ACS Omega, 2022, 7, 9388-9396.	3.5	17
3	Direct Conversion of Methane to C <sub>2</sub> Hydrocarbons in Solid-State Membrane Reactors at High Temperatures. Chemical Reviews, 2022, 122, 3966-3995.	47.7	23
4	Tuning of Shape, Defects, and Disorder in Lanthanum-Doped Ceria Nanoparticles: Implications for High-Temperature Catalysis. ACS Applied Nano Materials, 2022, 5, 8859-8867.	5.0	5
5	From thin films to shaped platelets: effects of temperature gradient on SnS synthesis. Thin Solid Films, 2021, 721, 138507.	1.8	4
6	Process of production of CVD graphene membrane for desalination and water treatment: a review of experimental research results. Brazilian Journal of Chemical Engineering, 2021, 38, 423-434.	1.3	3
7	Oxygen vacancy engineering of TaO <sub>x</sub> -based resistive memories by Zr doping for improved variability and synaptic behavior. Nanotechnology, 2021, 32, 405202.	2.6	6
8	Characterization and application of niobium-doped titanium dioxide thin films prepared by sol–gel process. Applied Physics A: Materials Science and Processing, 2021, 127, 1.	2.3	3
9	Alumina coating for dispersion management in ultra-high Q microresonators. APL Photonics, 2020, 5, 116107.	5.7	10
10	Buckypapers of carbon nanotubes and cellulose nanofibrils: Foldable and flexible electrodes for redox supercapacitors. Electrochimica Acta, 2020, 349, 136241.	5.2	25
11	Exsolution of Nickel Nanoparticles from Mixedâ€Valence Metal Oxides: A Quantitative Evaluation by Magnetic Measurements. Particle and Particle Systems Characterization, 2020, 37, 1900472.	2.3	6
12	Flash Sintering Samaria-Doped Ceria–Carbon Nanotube Composites. Ceramics, 2019, 2, 64-73.	2.6	17
13	Neurotoxicity in zebrafish exposed to carbon nanotubes: Effects on neurotransmitters levels and antioxidant system. Comparative Biochemistry and Physiology Part - C: Toxicology and Pharmacology, 2019, 218, 30-35.	2.6	32
14	A systematic study of multifunctional xTiO2/(100 â^' x)SiO2 thin films prepared by sol–gel process. Journal of Sol-Gel Science and Technology, 2019, 89, 380-391.	2.4	7
15	Probing the Electronic Properties of Monolayer MoS <sub>2</sub> via Interaction with Molecular Hydrogen. Advanced Electronic Materials, 2019, 5, 1800591.	5.1	22
16	High-yield synthesis of bundles of double- and triple-walled carbon nanotubes on aluminum flakes. Carbon, 2018, 133, 53-61.	10.3	14
17	Influence of substrate on the structure of predominantly anatase TiO <sub>2</sub> films grown by reactive sputtering. RSC Advances, 2018, 8, 7062-7071.	3.6	5
18	Monolayer and bilayer graphene on polydimethylsiloxane as a composite membrane for gasâ€barrier applications. Journal of Applied Polymer Science, 2017, 134, 45521.	2.6	10

#	Article	IF	CITATIONS
19	Oxide-cladding aluminum nitride photonic crystal slab: Design and investigation of material dispersion and fabrication induced disorder. Journal of Applied Physics, 2016, 119, .	2.5	3
20	Influence of annealing temperature and Sn doping on the optical properties of hematite thin films determined by spectroscopic ellipsometry. Journal of Applied Physics, 2016, 119, 245104.	2.5	9
21	The role of hydrogen partial pressure on the annealing of copper substrates for graphene CVD synthesis. Materials Research Express, 2016, 3, 045602.	1.6	20
22	Room temperature observation of the correlation between atomic and electronic structure of graphene on Cu(110). RSC Advances, 2016, 6, 98001-98009.	3.6	2
23	Synthesis of iron pyrite thin films by Russian Doll sulfurization apparatus. Thin Solid Films, 2016, 616, 303-310.	1.8	0
24	Nafion–titanate nanotubes composites prepared by in situ crystallization and casting for direct ethanol fuel cells. International Journal of Hydrogen Energy, 2015, 40, 1859-1867.	7.1	22
25	One-pot in situ photochemical synthesis of graphene oxide/gold nanorod nanocomposites for surface-enhanced Raman spectroscopy. RSC Advances, 2015, 5, 46552-46557.	3.6	18
26	Temperature dependence of the electrical properties of hydrogen titanate nanotubes. Journal of Applied Physics, 2014, 116, 184307.	2.5	3
27	Real time spectroscopic ellipsometry for analysis and control of thin film polycrystalline semiconductor deposition in photovoltaics. Thin Solid Films, 2014, 571, 442-446.	1.8	23
28	Oxidative desulfurization of dibenzothiophene over titanate nanotubes. Fuel, 2014, 132, 53-61.	6.4	78
29	Graphene chemical vapor deposition at very low pressure: The impact of substrate surface self-diffusion in domain shape. Applied Physics Letters, 2014, 105, .	3.3	13
30	Determination of the band alignment of multi-walled carbon nanotubes decorated with cadmium sulfide. Applied Surface Science, 2014, 321, 283-288.	6.1	4
31	Generation of reactive oxygen species in titanates nanotubes induced by hydrogen peroxide and their application in catalytic degradation of methylene blue dye. Journal of Molecular Catalysis A, 2014, 394, 316-323.	4.8	26
32	Applications of real-time and mapping spectroscopic ellipsometry for process development and optimization in hydrogenated silicon thin-film photovoltaics technology. Solar Energy Materials and Solar Cells, 2014, 129, 32-56.	6.2	19
33	Asymmetric Effect of Oxygen Adsorption on Electron and Hole Mobilities in Bilayer Graphene: Long- and Short-Range Scattering Mechanisms. ACS Nano, 2013, 7, 6597-6604.	14.6	34
34	Gene expression and biochemical responses in brain of zebrafish Danio rerio exposed to organic nanomaterials: Carbon nanotubes (SWCNT) and fullerenol (C60(OH)18–22(OK4)). Comparative Biochemistry and Physiology Part A, Molecular & Integrative Physiology, 2013, 165, 460-467.	1.8	30
35	<i>In Situ</i> Fabrication of Nafion–Titanate Hybrid Electrolytes for High-Temperature Direct Ethanol Fuel Cell. Journal of Physical Chemistry C, 2013, 117, 16863-16870.	3.1	23
36	Optimization of a-Si:H p-i-n solar cells through development of n-layer growth evolution diagram and		3

large area mapping. , 2013, , .

#	Article	IF	CITATIONS
37	Surface properties of oxidized and aminated multi-walled carbon nanotubes. Journal of the Brazilian Chemical Society, 2012, 23, 1078-1086.	0.6	97
38	Self-assembled films of multi-wall carbon nanotubes used in gas sensors to increase the sensitivity limit for oxygen detection. Carbon, 2012, 50, 1953-1958.	10.3	51
39	Synthesis and characterization of SnO2 thin films prepared by dip-coating method. Physics Procedia, 2012, 28, 22-27.	1.2	26
40	Enhanced electrochemical activity using vertically aligned carbon nanotube electrodes grown on carbon fiber. Materials Research, 2011, 14, 403-407.	1.3	7
41	Thermal behavior of carbon nanotubes decorated with gold nanoparticles. Journal of Thermal Analysis and Calorimetry, 2011, 105, 953-959.	3.6	18
42	Nafion-based composite electrolytes for proton exchange membrane fuel cells operating above 120 °C with titania nanoparticles and nanotubes as fillers. Journal of Power Sources, 2011, 196, 1061-1068.	7.8	57
43	New material for low-dose brachytherapy seeds: Xe-doped amorphous carbon films with post-growth neutron activated 1251. Applied Radiation and Isotopes, 2011, 69, 118-121.	1.5	9
44	Hydrogen sensing in titanate nanotubes associated with modulation in protonic conduction. Nanotechnology, 2011, 22, 235501.	2.6	8
45	Carbothermal reduction of the YSZ–NiO solid oxide fuel cell anode precursor by carbon-based materials. Journal of Thermal Analysis and Calorimetry, 2009, 97, 157-161.	3.6	10
46	Thermal properties of Nafion–TiO2 composite electrolytes for PEM fuel cell. Journal of Thermal Analysis and Calorimetry, 2009, 97, 591-594.	3.6	31
47	Nanostructured 3-D collagen/nanotube biocomposites for future bone regeneration scaffolds. Nano Research, 2009, 2, 462-473.	10.4	53
48	Fabrication of Gas Nanosensors and Microsensors via Local Anodic Oxidation. Langmuir, 2009, 25, 602-605.	3.5	12
49	On the growth and electrical characterization of CuO nanowires by thermal oxidation. Journal of Applied Physics, 2009, 106, .	2.5	139
50	Direct Production of Carbon Nanotubes/Metal Nanoparticles Hybrids from a Redox Reaction between Metal Ions and Reduced Carbon Nanotubes. ACS Applied Materials & Interfaces, 2009, 1, 2104-2106.	8.0	29
51	Vapor–Solid–Solid Growth Mechanism Driven by Epitaxial Match between Solid AuZn Alloy Catalyst Particles and ZnO Nanowires at Low Temperatures. Advanced Materials, 2008, 20, 1499-1504.	21.0	60
52	Deformation Induced Semiconductor-Metal Transition in Single Wall Carbon Nanotubes Probed by Electric Force Microscopy. Physical Review Letters, 2008, 100, 256804.	7.8	62
53	On the elastic constants of amorphous carbon nitride. Diamond and Related Materials, 2008, 17, 1850-1852.	3.9	2
54	Determination of the epitaxial growth of zinc oxide nanowires on sapphire by grazing incidence synchrotron x-ray diffraction. Applied Physics Letters, 2007, 90, 181929.	3.3	14

#	Article	IF	CITATIONS
55	Purity Evaluation of Carbon Nanotube Materials by Thermogravimetric, TEM, and SEM Methods. Journal of Nanoscience and Nanotechnology, 2007, 7, 3477-3486.	0.9	72
56	Mixed ionic-electronic conductivity in yttria-stabilized zirconia/carbon nanotube composites. Applied Physics Letters, 2007, 91, 243107.	3.3	11
57	Nafion–Titanate Nanotube Composite Membranes for PEMFC Operating at High Temperature. Journal of the Electrochemical Society, 2007, 154, B1358.	2.9	43
58	Chemical vapor deposition of multi-walled carbon nanotubes from nickel/yttria-stabilized zirconia catalysts. Applied Physics A: Materials Science and Processing, 2006, 84, 271-276.	2.3	28
59	Synthesis of Silica Nanowires by Active Oxidation of Silicon Substrates. Journal of Nanoscience and Nanotechnology, 2006, 6, 791-795.	0.9	7
60	Polymer Blend for Electrolyte and Electrode Coatings. Macromolecular Symposia, 2005, 229, 160-167.	0.7	3
61	Morphological and magnetic properties of carbon–nickel nanocomposite thin films. Journal of Applied Physics, 2005, 97, 044313.	2.5	43
62	Co-Sputtered Carbon-Nickel Nanocomposite Thin Films. Journal of Metastable and Nanocrystalline Materials, 2004, 20-21, 700-704.	0.1	4
63	Comparison of Phase Diagrams for vhf and rf Plasma-Enhanced Chemical Vapor Deposition of Si:H Films. Materials Research Society Symposia Proceedings, 2004, 808, 299.	0.1	3
64	Application of spectral and temporal weighted error functions for data analysis in real-time spectroscopic ellipsometry. Thin Solid Films, 2004, 455-456, 106-111.	1.8	8
65	Calibration and data reduction for a UV-extended rotating-compensator multichannel ellipsometer. Thin Solid Films, 2004, 455-456, 132-137.	1.8	22
66	Evaluation of compositional depth profiles in mixed-phase (amorphous+crystalline) silicon films from real time spectroscopic ellipsometry. Thin Solid Films, 2004, 455-456, 665-669.	1.8	28
67	Analytical model for the optical functions of amorphous semiconductors and its applications for thin film solar cells. Thin Solid Films, 2004, 455-456, 388-392.	1.8	36
68	Advances in multichannel ellipsometric techniques for in-situ and real-time characterization of thin films. Thin Solid Films, 2004, 469-470, 38-46.	1.8	6
69	Kinetics of silicon film growth and the deposition phase diagram. Journal of Non-Crystalline Solids, 2004, 338-340, 13-18.	3.1	18
70	Structural properties of amorphous carbon nitride films prepared by ion beam assisted deposition. Journal of Non-Crystalline Solids, 2004, 338-340, 486-489.	3.1	2
71	Evolution of microstructure and phase in amorphous, protocrystalline, and microcrystalline silicon studied by real time spectroscopic ellipsometry. Solar Energy Materials and Solar Cells, 2003, 78, 143-180.	6.2	305
72	Identification of the mechanism-limiting nitrogen diffusion in metallic alloys by in situ photoemission electron spectroscopy. Journal of Applied Physics, 2003, 94, 5435.	2.5	20

#	Article	IF	CITATIONS
73	Evolution of Crystallinity in Mixed-Phase (a+μc)-Si:H as Determined by Real Time Spectroscopic Ellipsometry. Materials Research Society Symposia Proceedings, 2003, 762, 5101.	0.1	4
74	Microstructure and Optical Functions of Transparent Conductors and their Impact on Collection in Amorphous Silicon Solar Cells. Materials Research Society Symposia Proceedings, 2003, 762, 1461.	0.1	2
75	Protocrystalline Si:H p-type Layers for Maximization of the Open Circuit Voltage in a-Si:H n-i-p Solar Cells. Materials Research Society Symposia Proceedings, 2002, 715, 611.	0.1	12
76	Maximization of the open circuit voltage for hydrogenated amorphous silicon n–i–p solar cells by incorporation of protocrystalline silicon p-type layers. Applied Physics Letters, 2002, 81, 1258-1260.	3.3	43
77	Analytical model for the optical functions of amorphous semiconductors from the near-infrared to ultraviolet: Applications in thin film photovoltaics. Journal of Applied Physics, 2002, 92, 2424-2436.	2.5	485
78	Extended phase diagrams for guiding plasma-enhanced chemical vapor deposition of silicon thin films for photovoltaics applications. Applied Physics Letters, 2002, 80, 2666-2668.	3.3	47
79	Phase diagrams for Si:H film growth by plasma-enhanced chemical vapor deposition. Journal of Non-Crystalline Solids, 2002, 299-302, 68-73.	3.1	6
80	Mobility gap profiles in Si:H intrinsic layers prepared by H2-dilution of SiH4: effects on the performance of p–i–n solar cells. Journal of Non-Crystalline Solids, 2002, 299-302, 1136-1141.	3.1	6
81	Advances in plasma-enhanced chemical vapor deposition of silicon films at low temperatures. Current Opinion in Solid State and Materials Science, 2002, 6, 425-437.	11.5	61
82	Light Induced Defect Creation Kinetics in Thin Film Protocrystalline Silicon Materials and Their Solar Cells. Materials Research Society Symposia Proceedings, 2002, 715, 1341.	0.1	52
83	Optical Simulations of the Effects of Transparent Conducting Oxide Interface Layers on Amorphous Silicon Solar Cell Performance. Materials Research Society Symposia Proceedings, 2001, 664, 2461.	0.1	6
84	Phase Diagrams for the Optimization of rf Plasma Enhanced Chemical Vapor Deposition of a-Si:H: Variations in Plasma Power and Substrate Temperature. Materials Research Society Symposia Proceedings, 2001, 664, 541.	0.1	11
85	Evolution of the Mobility Gap with Thickness in Hydrogen-Diluted Intrinsic Si:H Materials in the Phase Transition Region and Its Effect on p-i-n Solar Cell Characteristics. Materials Research Society Symposia Proceedings, 2001, 664, 1641.	0.1	11
86	Real Time Optics of p-Type Microcrystalline Silicon Deposition On Specular and Textured ZnO-Coated Glass. Materials Research Society Symposia Proceedings, 2000, 609, 1961.	0.1	7
87	Study of the Amorphous-to-Microcrystalline Transition during Silicon Film Growth at Increased Rates: Extensions of the Evolutionary Phase Diagram. Materials Research Society Symposia Proceedings, 2000, 609, 221.	0.1	15
88	Real time analysis of amorphous and microcrystalline silicon film growth by multichannel ellipsometry. Thin Solid Films, 2000, 364, 129-137.	1.8	42
89	Recent progress in thin film growth analysis by multichannel spectroscopic ellipsometry. Applied Surface Science, 2000, 154-155, 217-228.	6.1	42
90	Dependence of open-circuit voltage in hydrogenated protocrystalline silicon solar cells on carrier recombination in p/i interface and bulk regions. Applied Physics Letters, 2000, 77, 3093-3095.	3.3	50

#	Article	IF	CITATIONS
91	Evolutionary phase diagrams for the deposition of silicon films from hydrogen-diluted silane. Journal of Non-Crystalline Solids, 2000, 266-269, 43-47.	3.1	20
92	Modeling the dielectric functions of silicon-based films in the amorphous, nanocrystalline and microcrystalline regimes. Journal of Non-Crystalline Solids, 2000, 266-269, 269-273.	3.1	21
93	Optics of textured amorphous silicon surfaces. Journal of Non-Crystalline Solids, 2000, 266-269, 279-283.	3.1	15
94	Evolutionary phase diagrams for plasma-enhanced chemical vapor deposition of silicon thin films from hydrogen-diluted silane. Applied Physics Letters, 1999, 75, 2286-2288.	3.3	150
95	Real Time Optics of Amorphous Silicon Solar Cellfabrication on Textured Tin-Oxide-Coated Glass. Materials Research Society Symposia Proceedings, 1999, 557, 719.	0.1	6
96	Real Time Characterization of Non-Ideal Surfaces and Thin Film Growth by Advanced Ellipsometric Spectroscopies. Materials Research Society Symposia Proceedings, 1999, 569, 43.	0.1	2
97	Microcrystalline Silicon Tunnel Junctions for Amorphous Silicon-Based Multijunction Solar Cells. Materials Research Society Symposia Proceedings, 1999, 557, 579.	0.1	3
98	A NEW METHOD FOR STUDYING SEMICONDUCTING SURFACES IN AIR BY SCANNING TUNNELING MICROSCOPY. Modern Physics Letters B, 1996, 10, 1189-1195.	1.9	2
99	Contributions of bulk, interface and built-in potential to the open circuit voltage of a-Si:H solar cells. , 0, , .		2
100	The role of phase transitions between amorphous and microcrystalline silicon on the performance of protocrystalline Si:H solar cells. , 0, , .		3
101	Real time optics of p-type silicon deposition on specular and textured ZnO surfaces. , 0, , .		2
102	Effects of H/sub 2/-dilution and plasma power in amorphous silicon deposition: comparison of microstructural evolution and solar cell performance. , 0, , .		0
103	Microstructurally engineered p-layers for obtaining high open-circuit voltages in a-Si:H n-i-p solar cells. , 0, , .		5
104	Thickness evolution of the microstructural and optical properties of Si:H films in the amorphous-to-microcrystalline phase transition region. , 0, , .		4